Parameters	Specimen 1	Specimen 2
Acceleration voltage	90kV	
Radiographies numbers	1440	
Scan duration	~One hour	
Voxel size	6.35 µm	6.00 µm

Table 1 Key parameters of Lab-CT used for the characterizations of pores in the bulk of "Specimen 1 and 2"

Specimen		1	2
Loading conditions	**Max. stress (MPa)**	110	80~110
	R (Stress Ratio)	0.2	0.1~0.2
	Average max. strain	0.15%	0.10%
Results	**Crack initiation observed**	After 7000 c.	1st cycle (during initial tensile stage)
	Initiation site	Pore	Pore + Si (Possible)
	Propagation path	Hard inclusions (Si, iron intermetallics, copper containing phases)	
	Final failure (cycles)	≈ 100 000	20 430

Table 2 Basic loading conditions and results of tests

Pore	Feret diam. (mm)	Connection with the surface	Minimum distance to surface (mm)	
			Flat surface	Notched surface
A	1.31	Subsurface pore	0.18	0.02
B	1.37	Subsurface pore	0.80	0.90
C	0.90	Surface pore	0.00	1.70

Table 3 Size and location of Pore A, B and C shown in Fig. 8

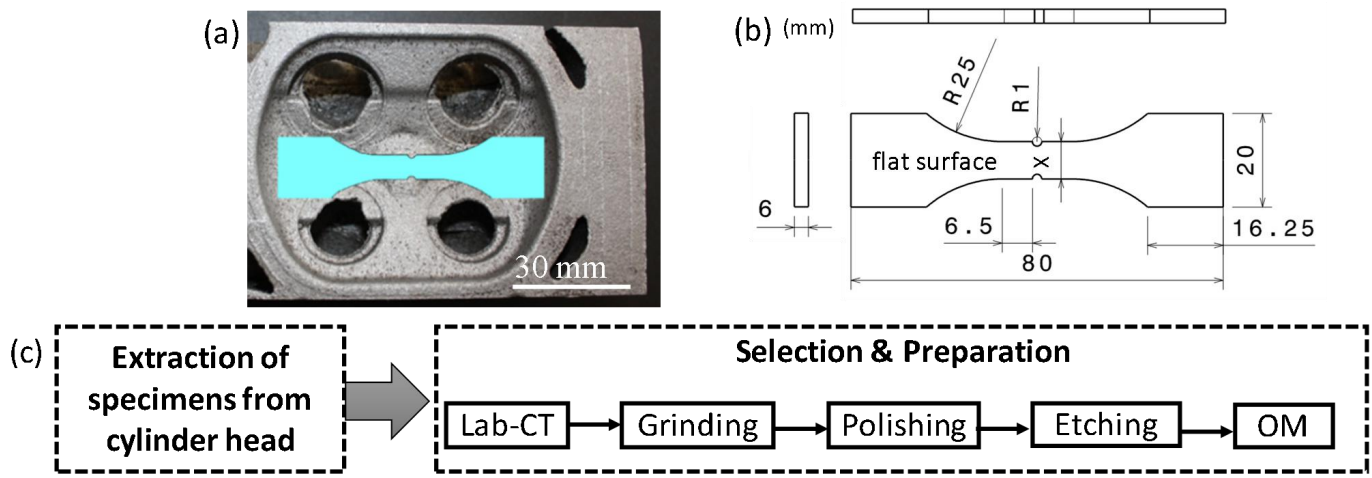

Fig. 1. (a) Extractions of specimens from cylinder head; (b) size in mm of extracted specimen ((X=10 (resp. = 8), K_t (Stress concentration factor) = 2.45 (resp. = 2.3) for Specimen 1 (resp. Specimen 2)); (c) the procedure of extraction, preparation of specimens and selection of ROI.

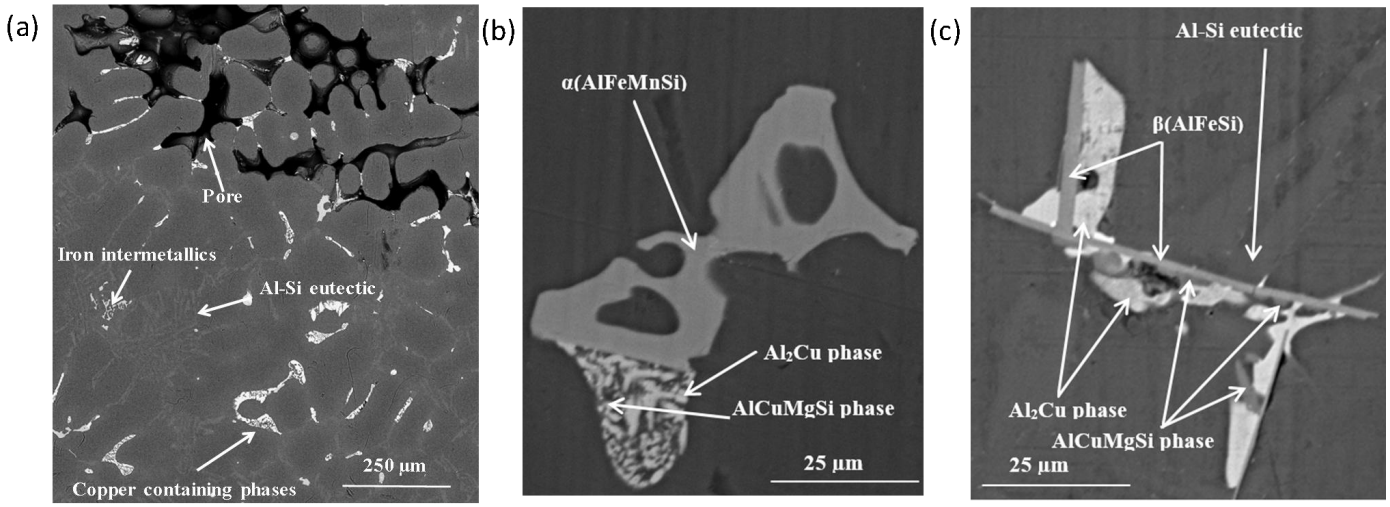

Fig. 2. 2D characterizations of LFC A319 alloy using SEM (BSE images): (a) an overview of the microstructural constituents; (b) and (c): higher resolution images reveal the details of iron intermetallics and copper containing phases.

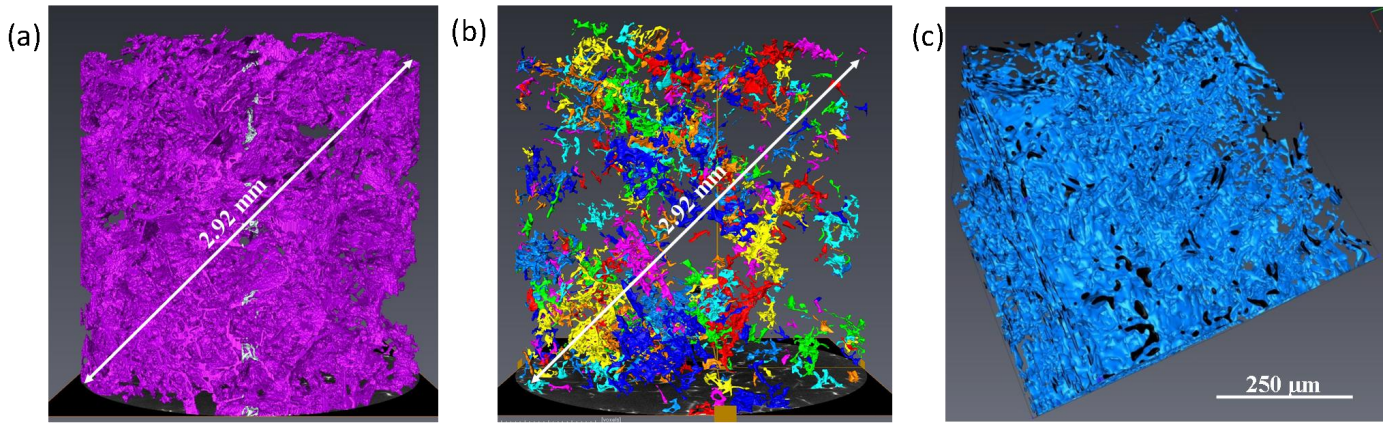

Fig. 3. 3D rendering of (a) iron intermetallics, (b) copper containing phases and (c) Si in LFC A319 alloy.

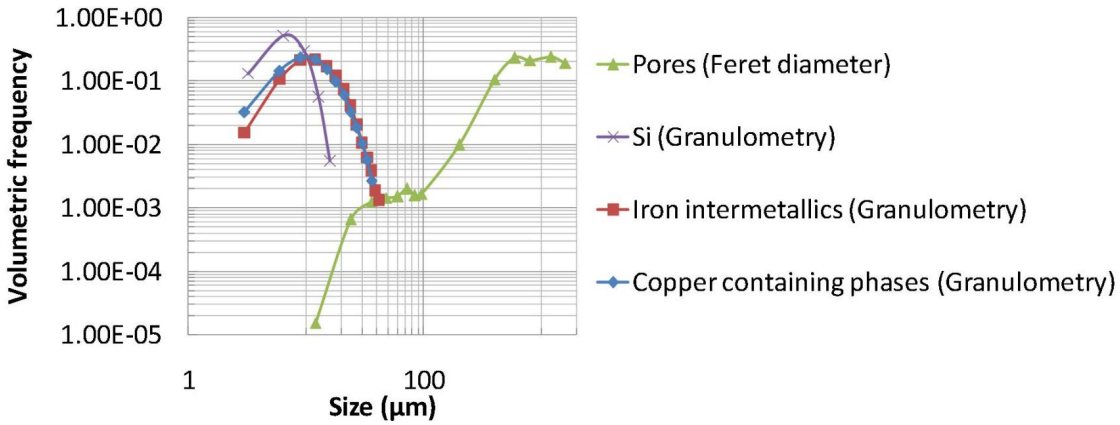

Fig. 4. Distributions of pores, and hard inclusions, i.e. Si, iron intermetallics and copper containing phases, as a function of size (Feret diameter for pores, granulometry for hard inclusions).

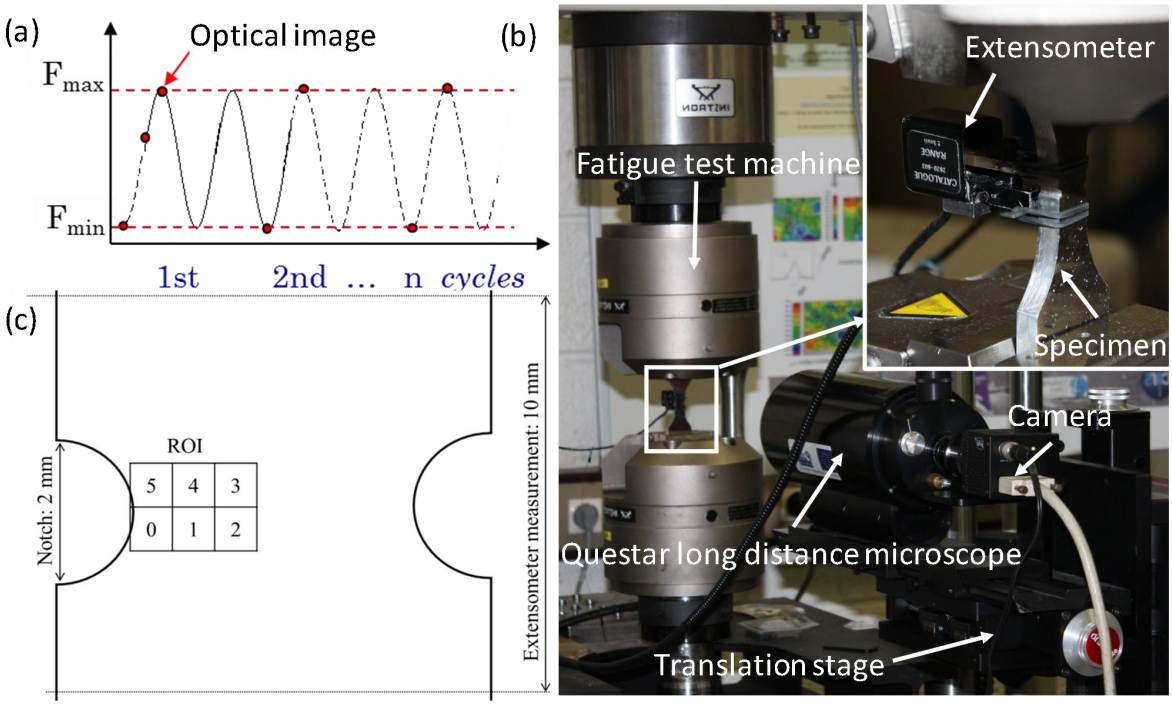

Fig. 5. (a) Scheme of images acquisition during fatigue tests; (b) fatigue tests with surface in-situ observations; (c) Schema of DIC measurement and extensometer measurement.

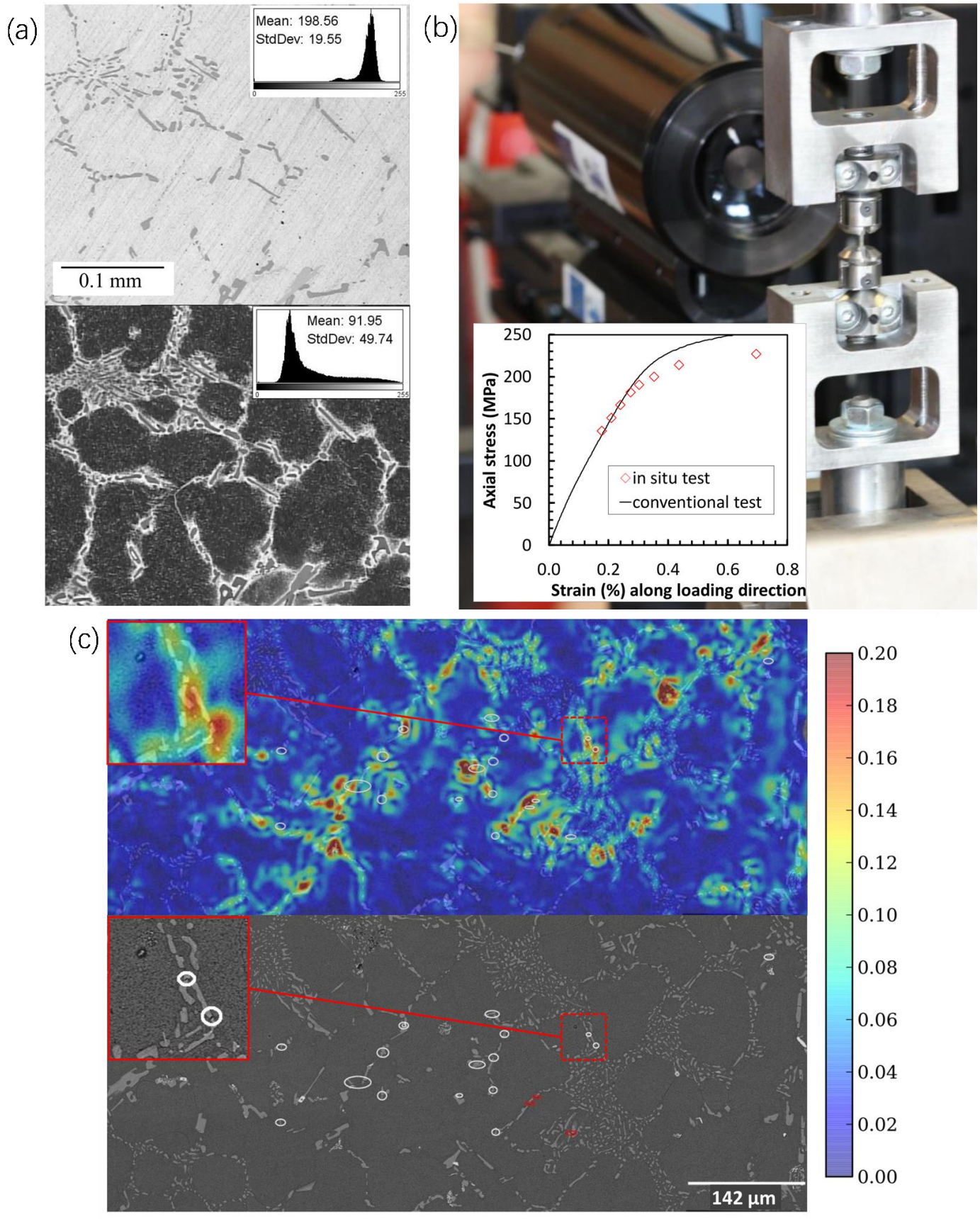

Fig. 6. (a) Optical microscopy images of the specimen surface before (top) and after (down) etching; histograms show the dynamic of the corresponding image in 8bit format; (b) Experimental set-up with Questar microscope; the stress-strain curve of the test is compared to that of a conventional test; (c) Cumulated strain field computed from DIC at the last load step before failure (237 MPa) and the corresponding SEM image showing fracture and debonding of Si particles; loading was along the vertical direction.

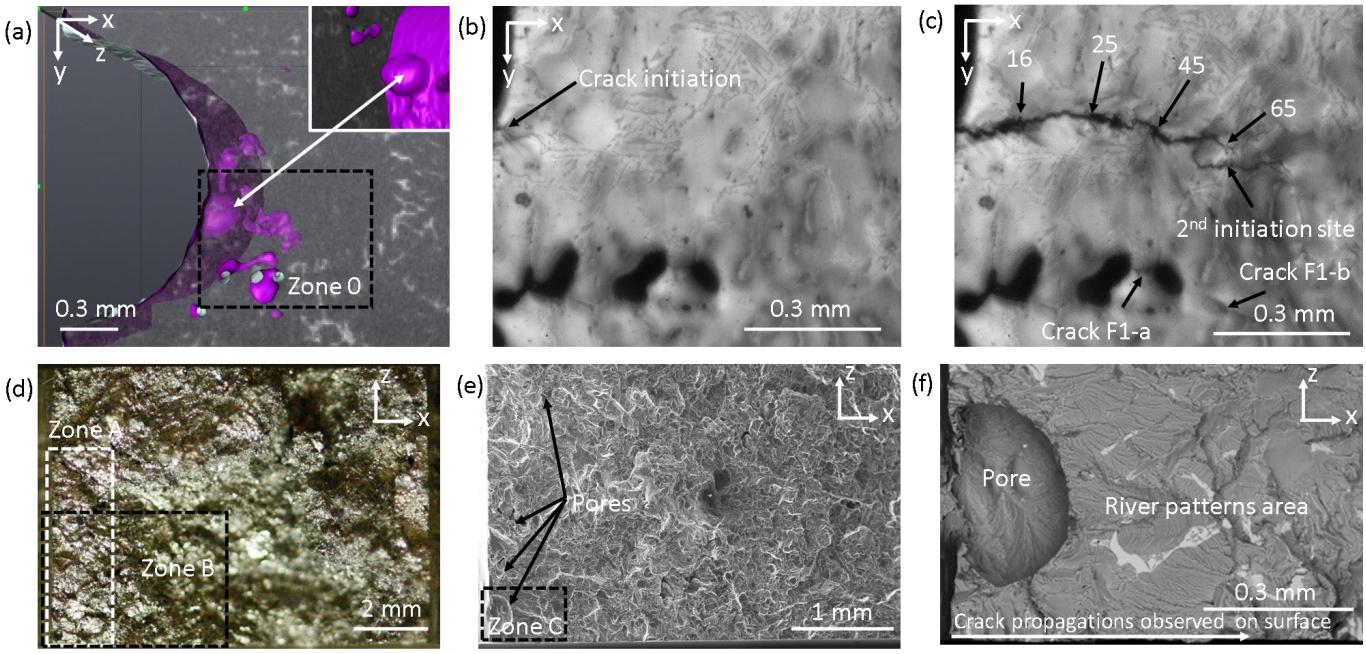

Fig. 7. Specimen 1: (a) 3D rendering of pores near the selected ROI on flat surface while the surface is set transparent; in-situ observation images captured after (b) 7000 cycles and (c) 90000 cycles in Zone 0 of (a), the arrows with number indicate the position of the arrested crack tip after the number of loading cycles shown in units of 1000; (d) whole fracture surface; (e) SEM image of Zone B in (d); (f) BSE image of Zone C in (e).

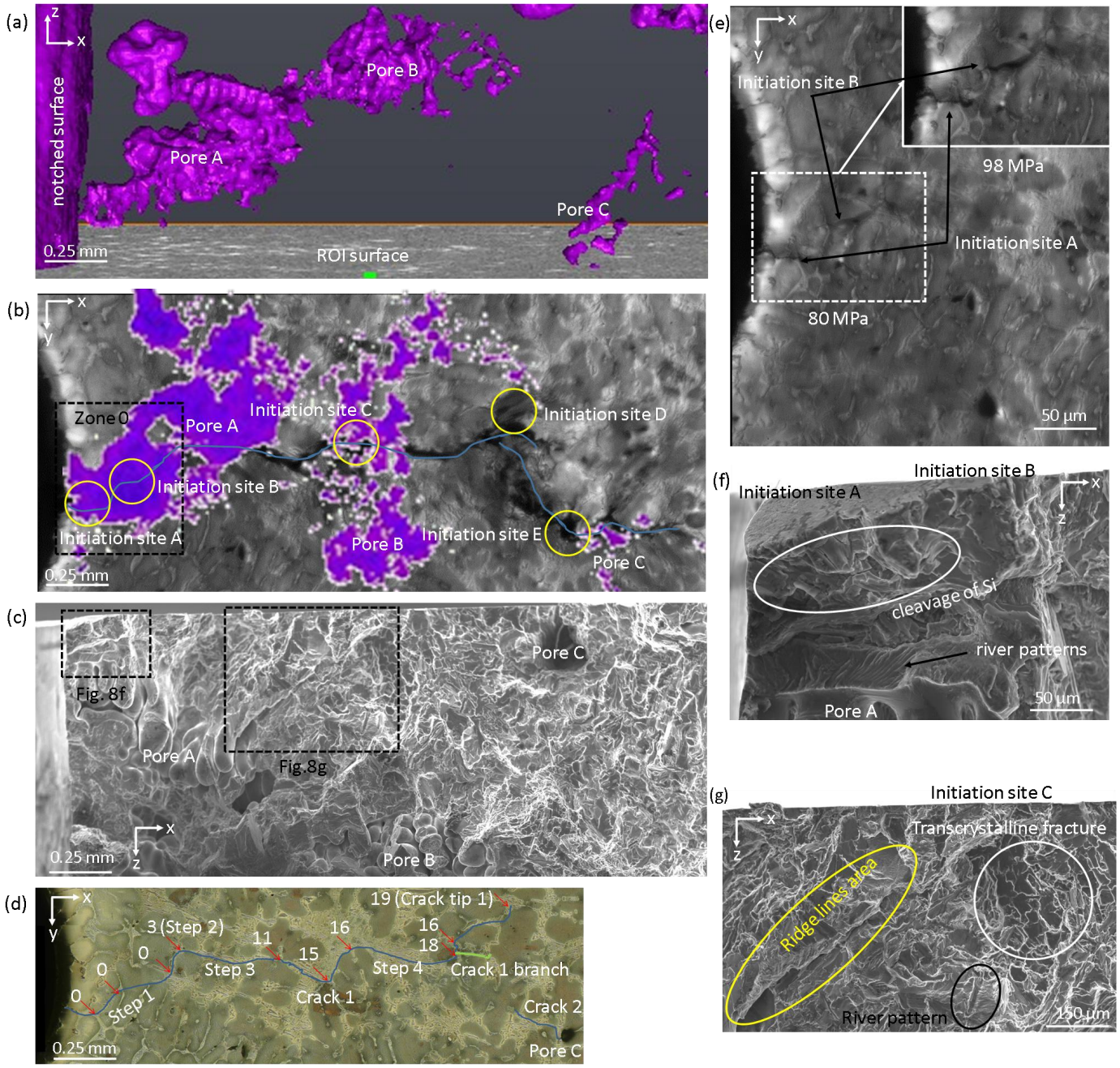

Fig. 8. Specimen 2: (a) 3D rendering of a cluster of pores below the selected ROI on surface; (b) in-situ observation image (stitched using six images) captured after 20300 cycles with the 2D projection of 3D pores from (a) shown in purple and final fracture marked with blue line; (c) the fracture surface observed by SEM in the corresponding area shown in (b); (d) OM image in ROI with the observed crack marked with lines and the arrows indicate the position of the crack tip after the number of loading cycles shown in units of 1000; (e) in-situ observation images captured during tensile stage of 1st cycle (Zone 0 in (b)); (f) (g) SEM image in the corresponding zones in (c).

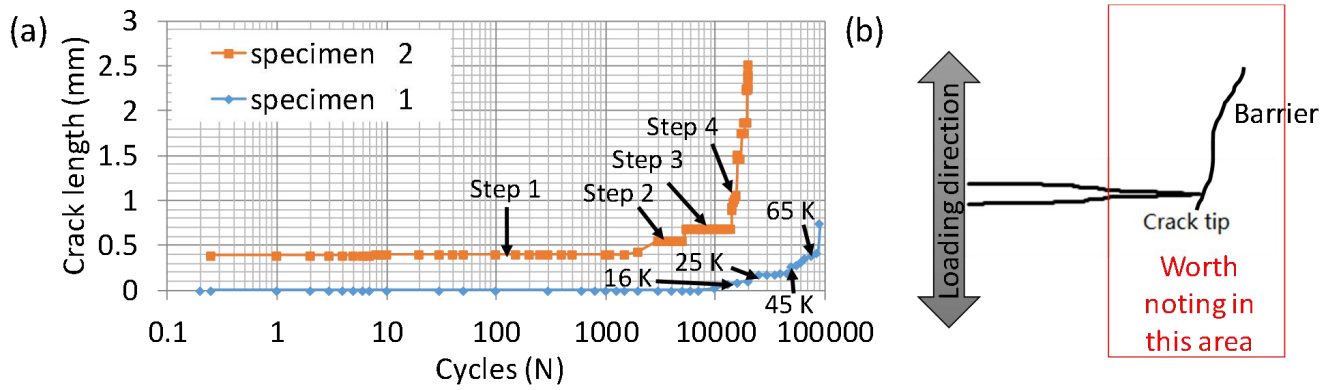

Fig. 9. (a) Crack length evolution with number of cycles; (b) schematic drawing of the area where crack tip is arrested by barrier.

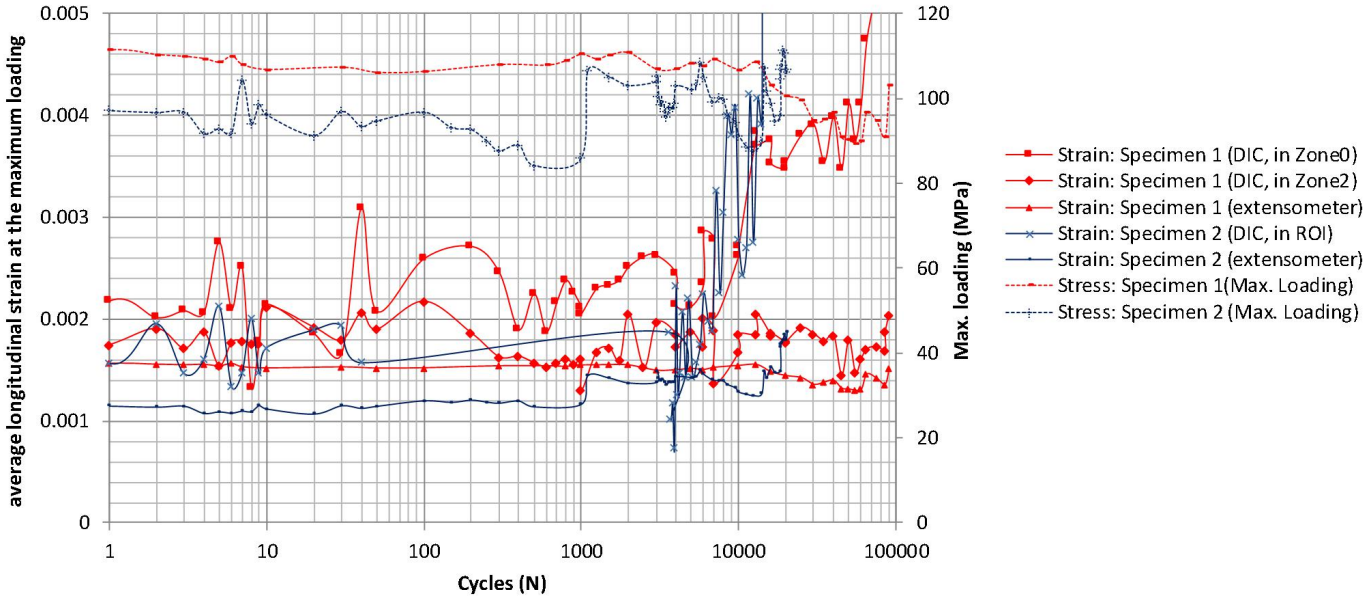

Fig. 10. Evolution of average longitudinal strain in Specimens 1 and 2, as measured by extensometer and DIC at the maximum load, with the number of cycles.

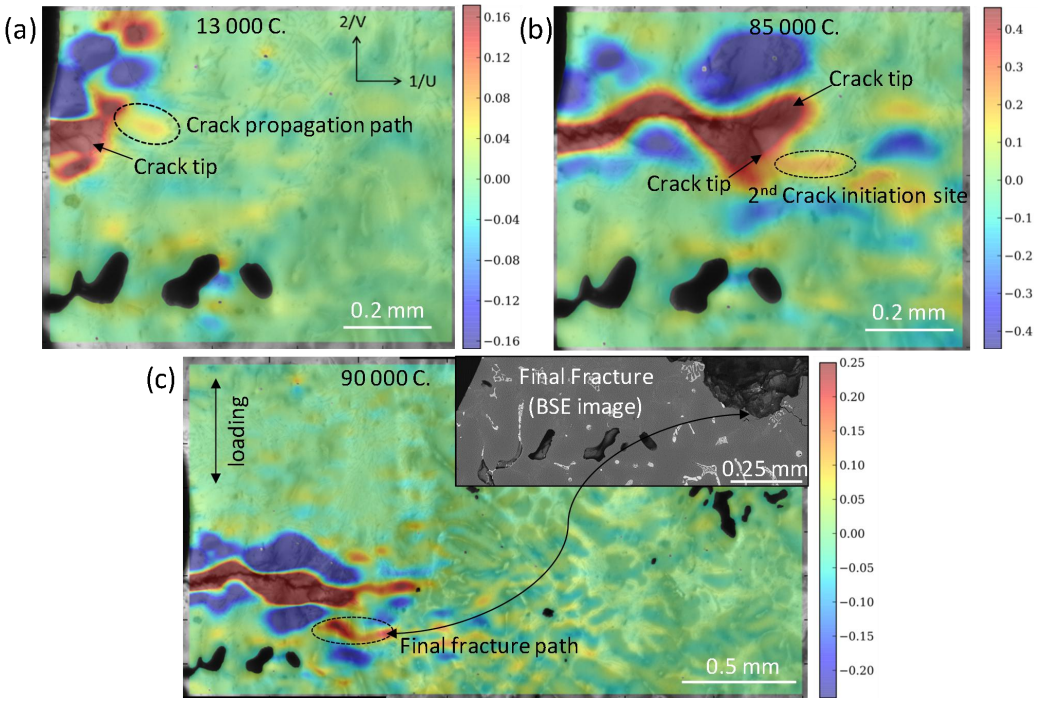

Fig. 11. DIC strain (ε22) measurement of Specimen 1: (a) 13 000 cycles and (b) 85 000 cycles in zone 0; (c) 90 000 cycles (last step before final failure) in the ROI shown with BSE image of final fracture in the top right.

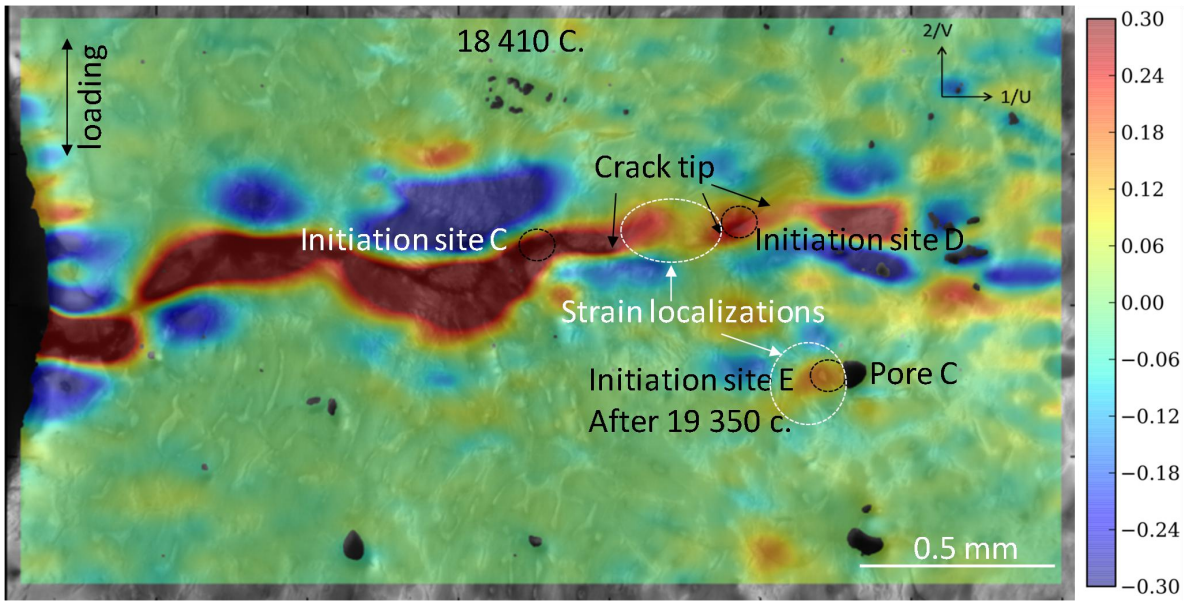

Fig. 12. DIC strain (ε22) measurement Specimen 2: 18 410 cycles in the ROI.